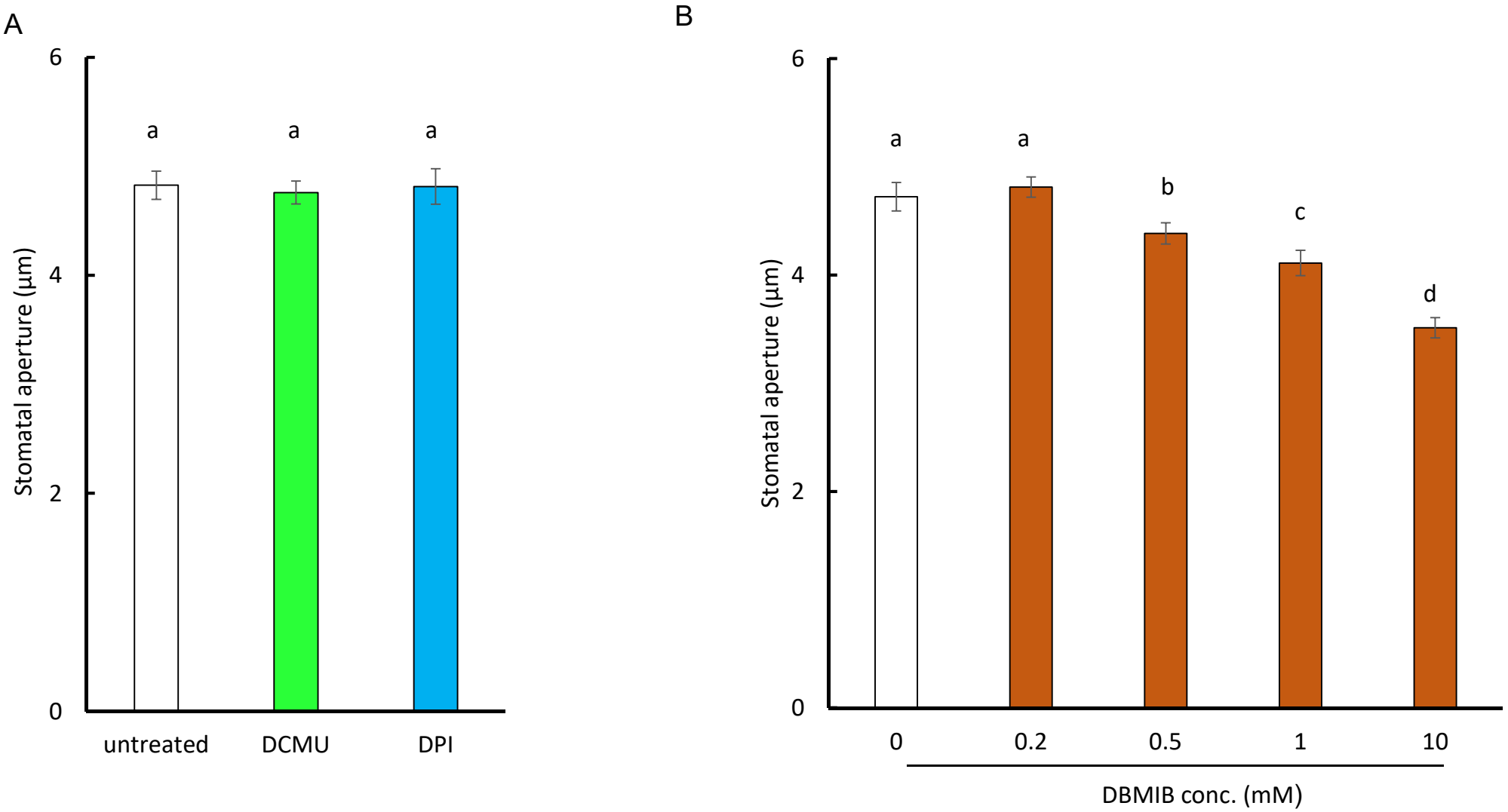

Figure S1. Effect of inhibitors on stomatal aperture in Arabidopsis.

(A) Effect of 10 µM DCMU and 10 µM DPI on the stomatal aperture. (B) Effect of DBMIB (0.2-10 µM) on the stomatal aperture.

Epidermal strips containing pre-opened guard cells were treated with DCMU, DPI or DBMIB for 2 hours. These experiments were conducted at 23°C in the light (50 µmol m^{-2} s^{-1}). Error bars represent standard error of the mean (n=100). Different letters indicate significant differences at $P < 0.05$.

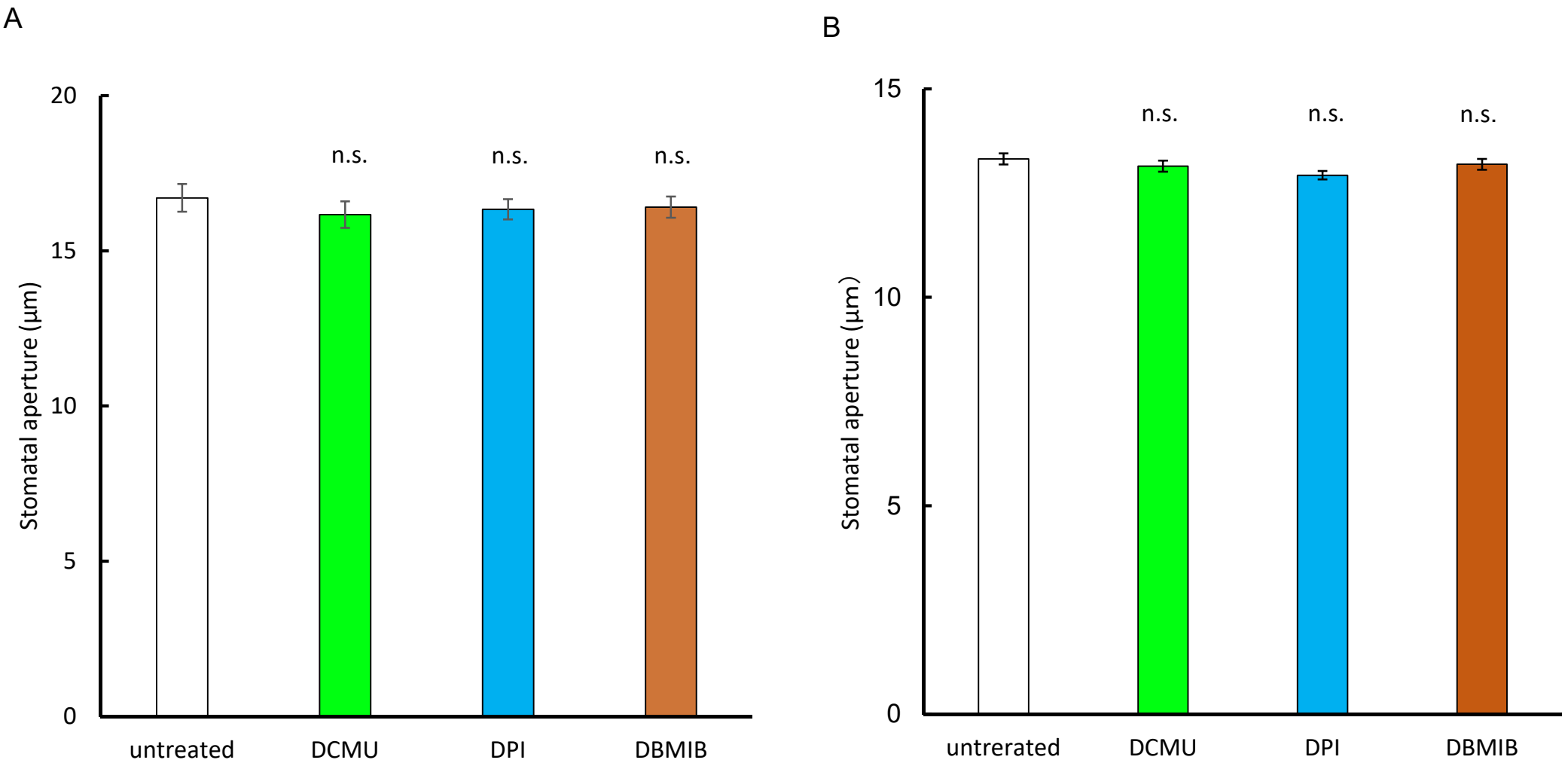

Figure S2. Effect of inhibitors on stomatal aperture in commelina and fava bean.
(A) commelia. (B) fava bean.

Epidermal strips containing pre-opened guard cells were treated with 10 μM DCMU, 10 μM DPI or 0.02μM DBMIB for 2 hours.
These experiments were conducted at 23°C in the light (50 μmol m^{-2} s^{-1}). Error bars represent standard error of the mean (n=100).
n.s.: The differences is not statistically significant with values for untreated cells.

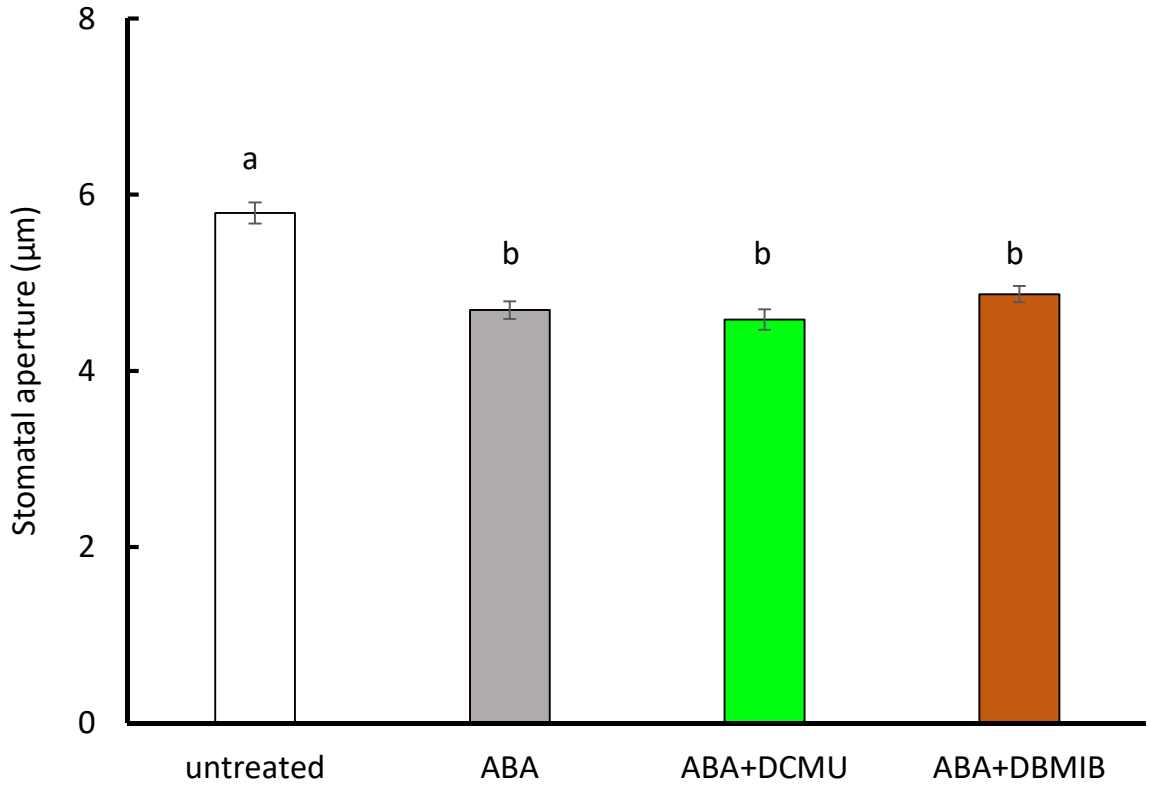

Figure S3. Photosynthetic inhibitors did not affect stomatal aperture in Arabidopsis when they were applied simultaneously with ABA.

Epidermal strips containing pre-opened guard cells were simultaneously treated with 10 µM ABA and 10 µM DCMU or 0.2 µM DBMIB for 2 hours. These experiments were conducted at 23°C in the light (50 µmol m^{-2} s^{-1}).
Error bars represent standard error of the mean (n=100). Different letters indicate significant differences at $P < 0.01$.

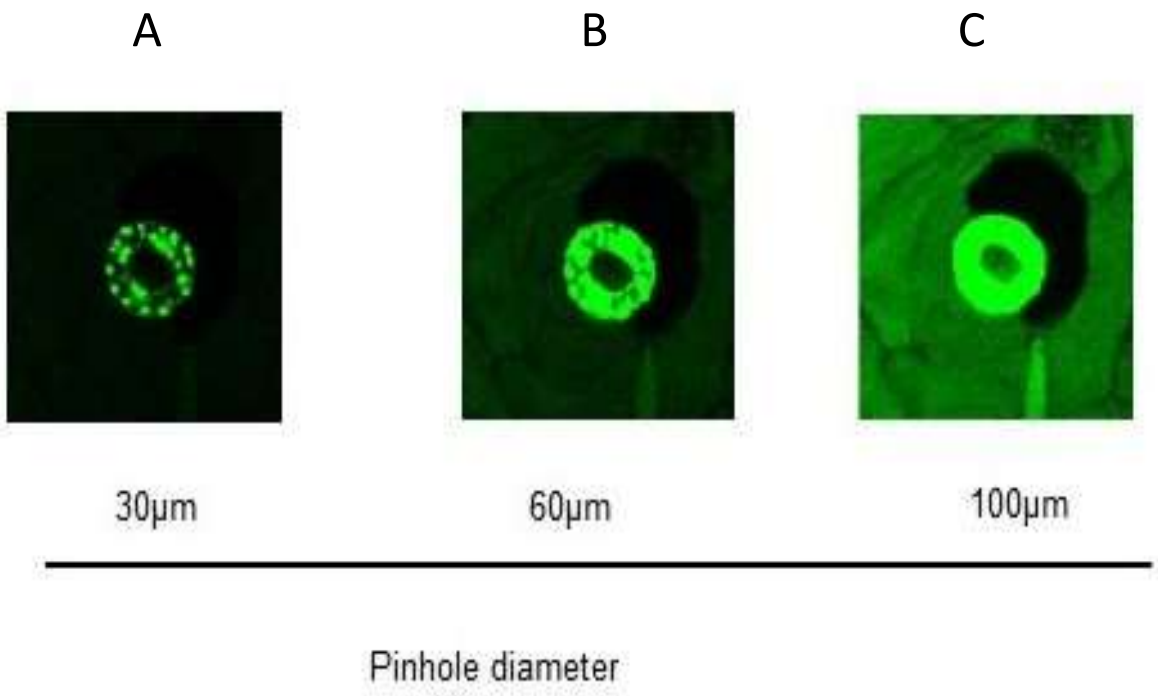

Figure S4. Effect of pinhole size on confocal micrographs.
(A) Fluorescence image acquired with small pinhole size of the excitation laser beam (30 µm).
(B) Fluorescence image acquired with middle pinhole size of the excitation laser beam (60 µm).
(C) Fluorescence image acquired with large pinhole size of the excitation laser beam (100 µm).

The epidermal strips were treated with 10 µM ABA for 5 min in the light and then treated with10 µM H_2DCFDA for 20 min in the dark. Confocal fluorescence images from H_2DCFDA were acquired with three different pinhole size of the excitation laser beam (30, 60 and 100 µm) in the same guard cell. The other conditions were the same among the three different micrographs.

A

B

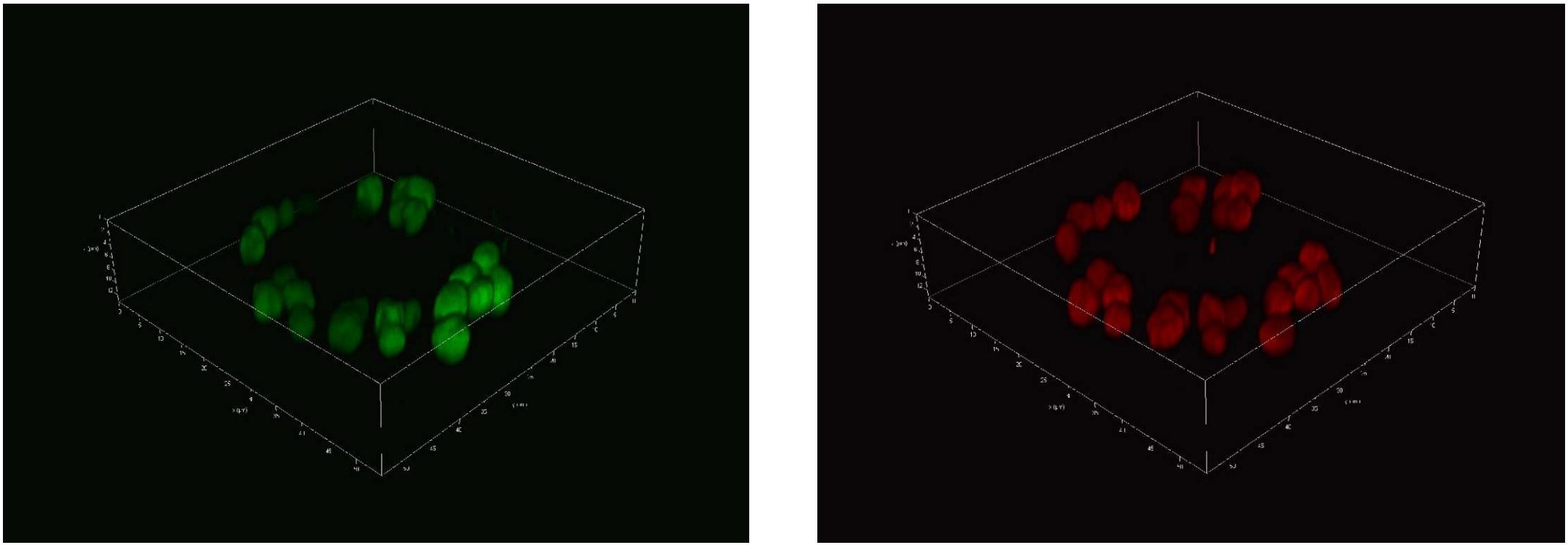

Figure S5. Three-dimensional (3D) images of ABA-induced reactive oxygen species and chloroplasts in guard cell of fava bean. (A) 3D-fluorescence image from H_2DCFDA. (B) 3D-fluorescence image from chloroplasts.

The epidermal strips were treated with 10 µM ABA for 5 min in the light and then treated with10 µM H_2DCFDA for 20 min in the dark. Fluorescence images were acquired with a Leica TCS SP8 confocal system (Leica Microsystems) equipped with HyD detectors using a 20x/0.40 numerical aperture oil immersion objective. For reactive oxygen species detection (fluorescence from H_2DCFDA), 495 nm white light laser was used for fluorophore excitation and the fluorescence were captured with HyD detector (505-550 nm). For chloroplast detection, 650 nm white light laser was used for fluorophore excitation and the fluorescence were captured with HyD detector (680-770 nm). The 3D pictures presented in the figures are projections from Z-stacks of 15 images with a *z*-step of 4 µm. The image data were processed using the LAS AF software.

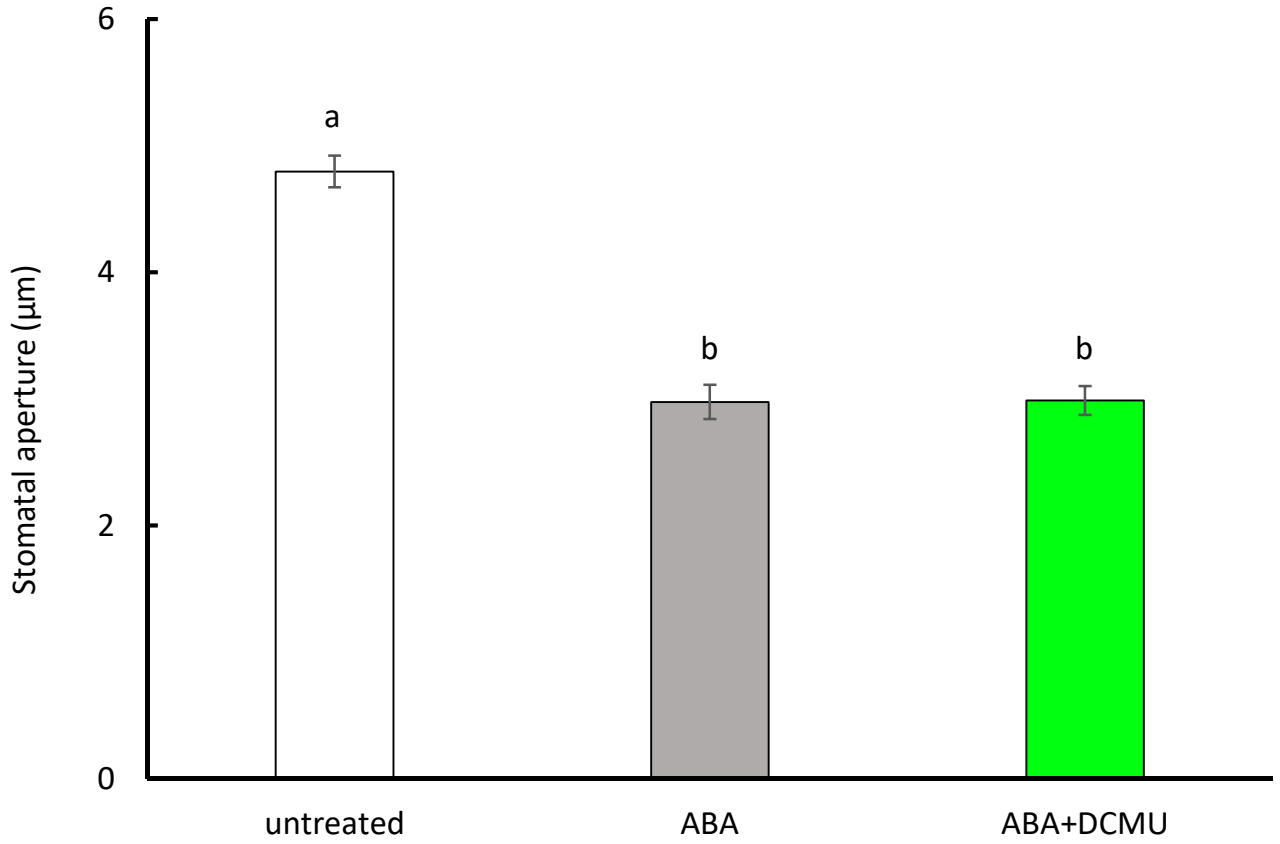

Figure S6. Effect of DCMU on ABA-induced stomatal closure using Arabidopsis leaves.

Leaves containing pre-opened guard cells were treated with 10 µM DCMU and 10 µM ABA for 2 hours.
These experiments were conducted at 23°C in the light (50 µmol m^{-2} s^{-1}).
Error bars represent standard error of the mean (n=100). Different letters indicate significant differences at $P < 0.01$.

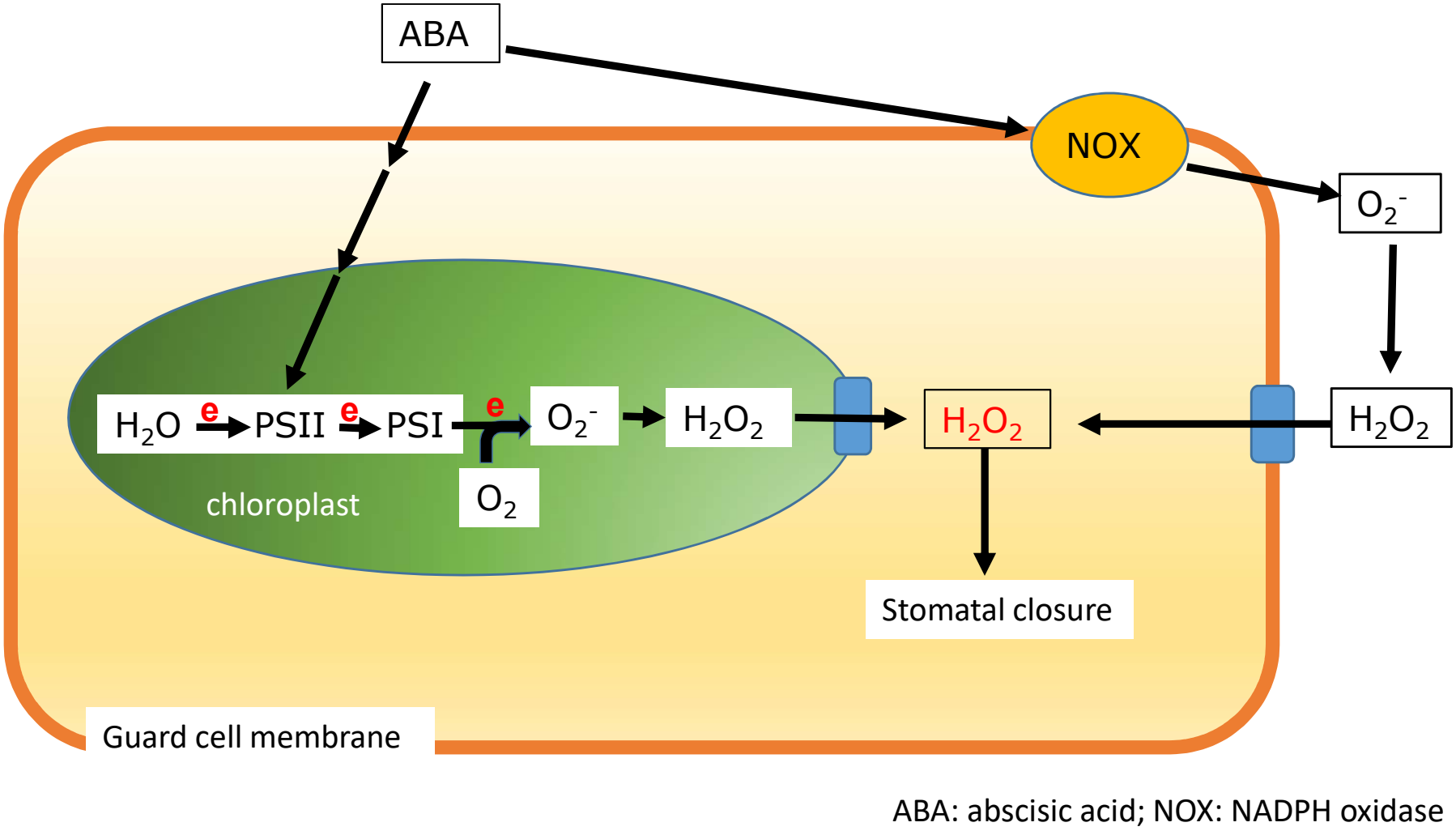

Figure S7. The proposed model of ABA-induced generation of reactive oxygen species (ROS) in guard cells.

There are two separate ABA-induced ROS generation pathways. (1) Under optimal condition for photosynthesis, light energy is converted to photosystem I by photosynthetic electron transport and the reduced PSI direct electron to NADPH which are spend for CO_2 fixation. In condition that ABA are added, NADPH/NADP ratio rise and NADP is shortage because unknown reason. The reduced photosystem I transfer electron to alternative electron acceptor, molecular oxygen, and generate ROS, such as superoxide anion and H_2O_2. (2) ABA activate plasma membrane bound-NADPH oxidase through SnRK protein kinase OST1 and elicit ROS in apoplast. These two pathways are contributed to ABA-induced ROS generation leading to stomatal closure.